Axion-Photon Coupling: Astrophysical Constraints

Oscar Straniero[1], *Adrián Ayala*[2,3], *Maurizio Giannotti*[4], *Alessandro Mirizzi*[5], *Inma Domínguez*[2]

[1]INAF-Osservatorio di Teramo, Teramo, Italy
[2]University of Granada, Granada, Spain
[3]University of Tor Vergata, Roma, Italy
[4]Barry University, Miami, USA
[5]University of Bari and INFN Bari, Bari, Italy

DOI: http://dx.doi.org/10.3204/DESY-PROC-2015-02/straniero_oscar

We revise the astrophysical bound to the axion-photon coupling, as obtained by comparing $R = N_{HB}/N_{RGB}$, the ratio of the numbers of stars observed in the Horizontal Branch (HB) and in the Red Giant Branch (RGB) of 39 Galactic Globular Clusters with up-to-date theoretical predictions. First results have already been published in a PRL paper in 2014. Here we present a new and more accurate method to calculate the theoretical R, which makes use of synthetic Color-Magnitude diagrams to be directly compared to the observed (real) diagrams. Preliminary results of our analysis are discussed.

1 Introduction

Globular Clusters (GC) are building blocks of any kind of galaxy. They are found in spirals (such as the Milky Way or M31), ellipticals (M87), as well as in Dwarfs Spheroidals or irregular galaxies (e.g. the Magellanic Clouds). Our Galaxy hosts hundreds of GCs. They are preferentially located in the Halo and in the Bulge. A typical GC contains between 10^5 and 10^7 almost coeval stars, as old as 13 Gyr, all linked together by reciprocal gravitational interactions. There exists a growing amount of observational evidences showing that GCs host multiple stellar populations, characterized by diverse chemical compositions.

In a color-magnitude diagram (CM diagram), stars belonging to the same cluster are grouped in distinct sequences (or branches), representing different evolutionary phases. For instance, in the Red Giant Branch (RGB) we find stars that are approching the He-burning phase: a He-rich and H-depleted core develops, rather high densities are attained, so that free electrons become highly degenerate. After the He ignition, these stars will move to the so-called Horizontal Branch (HB), the CM diagram location of core-He-burning stars. HB stars present an extended convective core, powered by the central He burning, surroundend by a semiconvective layer. A shell-H burning is always active in both RGB and HB stars. The number of stars observed in a given portion of the CM diagram is proportional to the time spent by a star in this region, e.g., $N_{RGB} \propto t_{RGB}$, where t_{RGB} is the RGB lifetime of a typical stars presently found in the RGB phase of a Galactic GC. Therefore, the ratio of the numbers of stars observed in the HB and in the RGB portion brighter than the zero-age HB[1], the so-called R parameter, represents

[1]It corresponds to the luminosity of the faintest HB stars.

the ratio of the respective stellar lifetimes:

$$R = \frac{N_{HB}}{N_{RGB}} = \frac{t_{HB}}{t_{RGB}} \tag{1}$$

R does not depend on metallicity and age of the cluster; however, R increases linearly with the He mass fraction (Y). For this reason, measurements of R in GCs have been largely used to estimate the pristine He content of our Galaxy. However, this method requires a detailed knowledge of the stellar lifetimes, usually obtained by means of stellar models. In practice, it relies on our knowledge of all the physical processes that produce or dissipate energy in stellar interiors, such as, for instance, the nuclear reactions or the thermal neutrino energy loss. On the other hand, if the GC He content is known, the R parameter measurements may be used to constrain these physical processes. On this basis, Ref. [4] investigated the axion production by the Primakov process, possibly occurring in the hot stellar interior. By comparing the t_{HB}/t_{RGB} derived from up-to-date stellar models of RGB and HB stars with the average R parameter of a sample of 39 galactic GCs with metallicity [Fe/H]< -1.1 ($R = 1.39 \pm 0.03$), we were able to put a rather strong upper bound for the axion-photon coupling, namely $g_{a\gamma} < 0.66 \times 10^{-10}$ GeV^{-1} (95% C.L.).

2 A step forward

More recently we have developed a new tool to generate *synthetic* CM diagrams. It is based on a more extended set of stellar models and allows us to plot perfect theoretical counterparts of real CM diagrams. For instance, stochastic variations of the position of the points representing stars, such as those due to the mass loss or to the photometric errors, are easily accounted for.

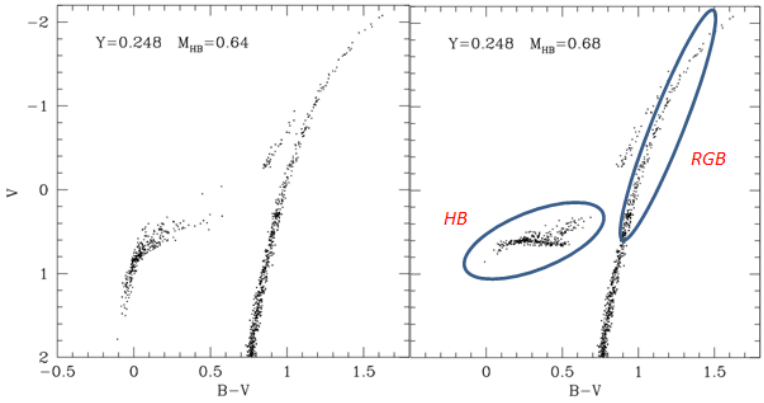

Figure 1: Example of synthetic CM diagrams. The diagram in the left panel has been obtained by assuming a stronger average mass loss rate during the RGB. As a result, the mean mass of HB stars (M_{HB}) is lower than that of the diagram in the right panel. The HB and the RGB portions used in the calculation of the R parameter are surrounded by ellipses.

In this way, we may calculate the *theoretical* R parameter by counting the stars (or their models) found in different branches of the synthetic CM diagram, precisely as we do for real

Parameter	error	Reference
$^{14}\mathrm{N}(p,\gamma)^{15}\mathrm{O}$	7%	[1]
$^{4}\mathrm{He}(2\alpha,\gamma)^{12}\mathrm{C}$	10%	[2]
$^{12}\mathrm{C}(\alpha,\gamma)^{16}\mathrm{O}$	20%	[6]
R	1.39 ± 0.03	[4]
Y	0.255 ± 0.002	[5],[3]

Table 1: List of the 5 parameters varied in the Monte Carlo analysis described in section 3. The first three rows refer to the rates of the 3 more relevant nuclear reactions that directly affect the lifetimes of HB and RGB stellar models. The fourth and the fifth rows contain the average R parameter of the 39 Cluster sample and the initial He mass fraction, respectively. The adopted 1σ errors and the sources of the measurements are listed in columns 2 and 3, respectively.

GCs. A first advantage of this method is that it allows us to reduce or eliminate some systematic uncertainties, such as those due to the determination of the zero-age HB. In addition, we may also estimate the uncertainty due to statistical fluctuations of the photometric sample. At the same time, we may also estimate the influence on the calculated R parameter of all the uncertainties of the stellar models. In particular, we have investigated the uncertainties due to nuclear reaction rates (RGB and HB models), convection (HB models), rate of energy-loss by plasma neutrino (RGB models) and some others. Examples of synthetic CM diagrams are shown in Figure 1.

3 Results

Although our analysis is still in progress, in this section we present some preliminary results. To combine all the uncertainties and obtain the propagation of their errors into the estimated upper bound for the axion-photon coupling, we have used a Monte Carlo method (MC): a sequence of synthetic CM diagrams are generated, each time with a different set of values for the parameters affected by the major uncertainties. The MC generates each set of parameters according to their errors. As an example, here we have considered variations of 5 parameters, namely, the 3 more relevant nuclear reaction rates, the He mass fraction (Y) and the measured R. The assumed values of these 5 parameters and the respective references are reported in Table 1.

Figure 2 illustrates the result of the MC. The axion-photon coupling ($g_{a\gamma}$) depends on the difference between the theoretical R_{th} (computed without axion energy loss) and the measured R_{GCs}: $\theta = R_{th} - R_{GCs}$. Note that R_{th} depends on Y and the 3 relevant reaction rates (see Table 1). In practice, we find that: $g_{a\gamma} = \alpha\theta^2 + \beta\theta$.

4 Conclusions

By means of synthetic CM diagrams, we have calculated the relation between $g_{a\gamma}$ and 5 parameters, namely Y, R, and the 3 more relevant nuclear rates affecting the HB and the RGB lifetimes. By combining the uncertainties on this 5 parameters we find $g_{10} = 0.29 \pm 0.18$, where

$g_{10} = g_{a\gamma}/10^{-10}\mathrm{GeV}^{-1}$, corresponding to an axion-photon upper bound (95% C.L.):

$$g_{10} < 0.65 \tag{2}$$

which confirms our previous finding [4].

The main source of uncertainty of the model is the $^{12}\mathrm{C}(\alpha,\gamma)^{16}\mathrm{O}$ reaction rate. This uncertainty is due to the possible interference between two subthreshold resonances in the $^{16}\mathrm{O}$ ($j^\pi = 1^-,\ 2^+$). Presently available measurements seem to exclude a constructive interference (enhanced rate). However, a destructive interference cannot be excluded yet. It this case, the reaction rate would be reduced down to the 50% of the most probable value. It would imply a systematic decrease of the theoretical R, thus reducing or even cancelling the apparent need of an additional cooling process. New low-energy measurements are required for this important nuclear process. A second issue concerns the adopted He mass fraction. Direct measurements of He abundances are very difficult for Globular Cluster stars, because their atmospheres are too cool to excite He atoms. Alternatively, we have used precise measurements of He abundances in extragalactic HII molecular regions (see Table 1) whose metallicity is in the same range of the galactic GCs. In general, it is expected that these environments experienced a limited chemical evolution (as the low metallicity testifies), so that their Y should be close to the primordial one. Note that the value of Y obtained from low-Z HII clouds is in tension with the standard prediction of primordial nucleosynthesis calculations and with results of the latest CMB analysis from the PLANCK collaboration. Note that with a lower Y, the need of an additional energy sink in HB stars disappears.

Summarizing, while the upper bound for the axion-photon coupling, as derived from the analysis of the R parameters of galactic GCs, is a firm result, the occurrence of a measured R lower than that predicted by stellar models (without axion energy loss) cannot be considered a proof of the existence of these particles.

References

[1] Adelberger, E. G., García, A., Robertson, R. G. H. et al., Reviews of Modern Physics **83**, 195 (2011).

[2] Angulo, C. et al., Nuclear Physics A **3**, 656 (1999).

[3] Aver, E., Olive, K. A., & Skillman, E. D., JCAP **7**, 011 (2015).

[4] Ayala A., Domínguez I., Giannotti M., Mirizzi A. & Straniero O., Phys. Rev. Lett. **113**, 191302 (2014).

[5] Izotov, Y. I., Thuan, T. X., & Guseva, N. G., MNRAS, **445** 778 (2014).

[6] Schürmann, D., Gialanella, L., Kunz, R. & Strieder, F., Physics Letters B, **35** 711 (2012).

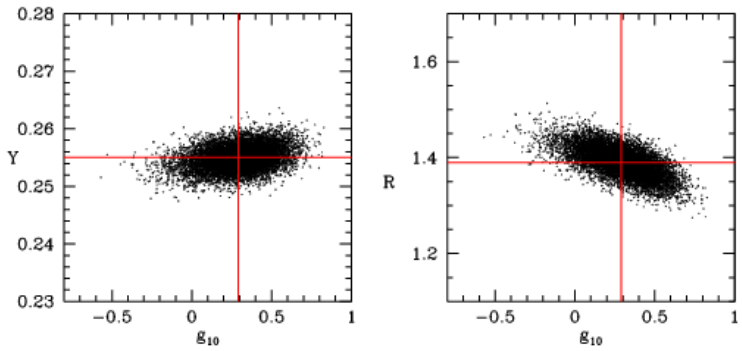

Figure 2: Monte Carlo results. These plots show the values of g_{10} as obtained by varying the 5 parameters listed in Table 1 as a function of two of them, i.e. the Globular Cluster R parameter (right panel) and the He mass fraction (Y, left panel). R and Y are varied according to a normal error function with the 1σ errors reported in column 2 of Table 1. Similar plots may be obtained for the 3 most relevant nuclear reaction rates.